JACS
JOURNAL OF THE AMERICAN CHEMICAL SOCIETY
pubs.acs.org/JACS
Article

# Regulating DNA-Hybridization Using a Chemically Fueled Reaction Cycle

Michele Stasi, Alba Monferrer, Leon Babl, Sreekar Wunnava, Christina Felicitas Dirscherl, Dieter Braun, Petra Schwille, Hendrik Dietz, and Job Boekhoven*

Cite This: https://doi.org/10.1021/jacs.2c08463
Read Online
ACCESS | Metrics & More | Article Recommendations | Supporting Information

**ABSTRACT:** Molecular machines, such as ATPases or motor proteins, couple the catalysis of a chemical reaction, most commonly hydrolysis of nucleotide triphosphates, to their conformational change. In essence, they continuously convert a chemical fuel to drive their motion. An outstanding goal of nanotechnology remains to synthesize a nanomachine with similar functions, precision, and speed. The field of DNA nanotechnology has given rise to the engineering precision required for such a device. Simultaneously, the field of systems chemistry developed fast chemical reaction cycles that convert fuel to change the function of molecules. In this work, we thus combined a chemical reaction cycle with the precision of DNA nanotechnology to yield kinetic control over the conformational state of a DNA hairpin. Future work on such systems will result in out-of-equilibrium DNA nanodevices with precise functions.

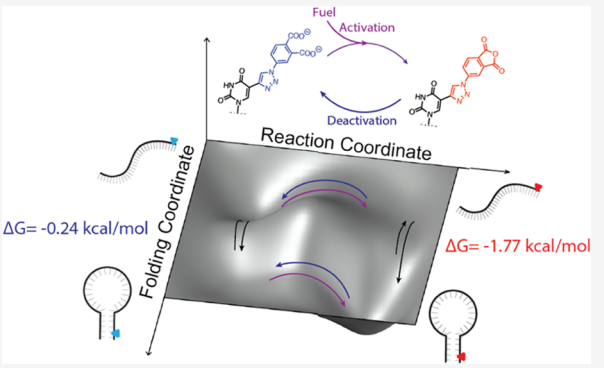


## INTRODUCTION

Nucleic acids have proven to be outstanding building blocks for molecular self-assembly. The precision and fidelity of base-pairing allow for predicting self-assembly patterns and optimizing the strength of the interaction. The advent of DNA origami[1−4] has pushed further the boundaries of the possible structures designed with DNA, opening the door for the easy bottom-up assembly of user-defined three-dimensional structures with unprecedented accuracy. Although initial works in the field have mainly focused on developing static structures, the so-called structural DNA nanotechnology, a strong interest is now diverted toward developing dynamic systems that reshape and actively interact with their surroundings.[5−8]

If structural DNA nanotechnology enables virtually building of any architecture on the nanometer scale, the combination with actuation mechanisms could fulfill the dream of a fully synthetic biomolecular machine.[7,9,10] Several strategies to control the actuation of DNA nanodevices have been employed. Toehold-mediated strand displacement reaction[11−17] is a popular approach that relies on user-designed DNA sequences with partial complementarity, making it easy to implement. A limiting factor in this strategy is the second-order kinetic hybridization between DNA sequences that require high concentrations of DNA strands to achieve operational speed in seconds. Alternative approaches for actuation of DNA-based nanodevices include light-responsive molecules,[18] redox stimuli,[19,20] pH-dependent secondary structures,[21−23] actuation by variating the ionic strength of the medium[24] or the temperature and thus controlling the stacking interaction of nucleobases in blunt ends,[8] through the use of external electric or magnetic fields,[9,25,26] or biomolecules such as antibodies[27] and enzymes.[28−31] Most of these strategies, except for the enzyme-driven ones, proceed stepwise, *i.e.*, the structure switches from one static state to another upon application of the stimulus. Additionally, they operate profoundly differently than naturally occurring biomolecular machines in harnessing the energy required to function. Specifically, the actuation process in dynamic DNA nanotechnology results from a change in the overall energy landscape (*e.g.*, by changing the pH or ionic strength), thereby driving the system into the new global minimum. Conversely, natural molecular machines, such as ATPases or motor proteins, couple the catalysis of a chemical reaction, *e.g.*, the hydrolysis of nucleotide triphosphates, to their conformational change: they incessantly consume fuel to drive their motion.[32] Recently, Del Grosso and co-workers introduced the concept of dissipative DNA nanotechnology to distinguish those systems that do not strictly operate under thermodynamic

Received: August 9, 2022

Downloaded via 46.183.103.8 on November 29, 2022 at 06:02:42 (UTC).
See https://pubs.acs.org/sharingguidelines for options on how to legitimately share published articles.

ACS Publications
© XXXX The Authors. Published by American Chemical Society

control but instead require the presence of an additional element: a chemical reaction as an energy-dissipative element.[33] The examples reported rely on ATP-consuming enzymes to ligate and excise DNA strands, thereby controlling their hybridization behavior[30,34−36] or RNases to degrade RNA strands.[29,37]

Outside of dissipative DNA nanotechnology, the constant conversion of fuels to drive the function of molecules has been successfully applied to the self-assembly of small molecules.[38,39] In such a chemically fueled system, molecular assembly is regulated by a fuel-driven reaction cycle that comprises at least two reactions, *i.e.*, an activation and deactivation reaction. In the activation reaction, a precursor reacts with a chemical fuel which activates it for self-assembly. In the deactivation, the activated product spontaneously reverts to the precursor. In its finite lifetime, the activated product can be temporarily part of a dynamic assembly, which is thus regulated by the kinetics of the reaction cycle. This strategy has resulted in chemically fueled dynamic fibers,[40,41] droplets,[42] and colloids.[43] More recently, chemically fueled reaction cycles have also been used to operate small molecular machines and motors.[44−46] Developments in chemically fueled self-assembly have resulted in fast reaction cycles in which activated products have half-lives of tens of seconds. Nevertheless, chemically fueled self-assembly of small molecules still lacks precision and designability compared to DNA nanotechnology.

In this work, we combined a fast reaction cycle with the precision of DNA nanotechnology to achieve kinetic control over the conformational state of a DNA hairpin (Scheme 1).

**Scheme 1. Schematic Representation of a Fuel-Driven Hairpin**[a]

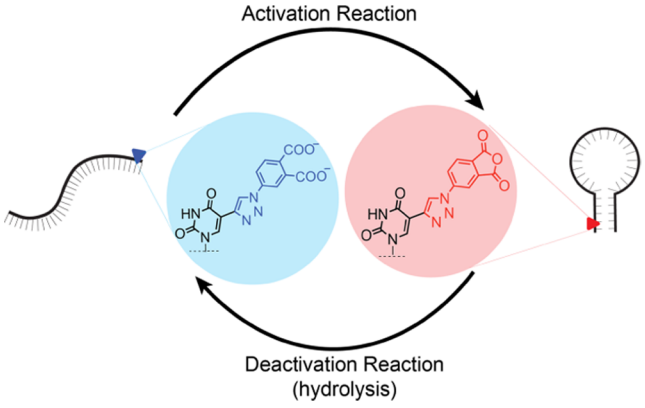


[a]The hairpin is mostly unfolded in its precursor state (dicarboxylic acid, blue). The folded state becomes more stable upon activation (anhydride, red).

We harness the energy of hydration of carbodiimide to shift the population of hybridized DNA versus single-stranded DNA. We reach a distribution not allowed at thermodynamic equilibrium. The system spontaneously reverts to its initial state once the fuel is fully consumed, and the nonequilibrium distribution cannot be further sustained. Our molecular design is versatile, can be quickly introduced in commercially available DNA sequences, and provides a strategy for nonequilibrium self-assembly and actuation in DNA nanotechnology. We demonstrate its applicability in both a unimolecular and a bimolecular setting, i.e., develop a strategy for chemically fueled strand displacement reaction based entirely on an abiotic fuel, potentially orthogonal to previously reported strategies.

## RESULTS AND DISCUSSION

We used a versatile, well-described chemical reaction cycle[47−49] in which a phthalic acid-based precursor is transiently activated into its corresponding anhydride at the expense of a molecule of EDC (1-ethyl-3-(3-dimethylaminopropyl)carbodiimide, Figure 1A). In the activation reaction, the precursor reacts with EDC to yield the precursor's anhydride state and EDU (1-(3-(dimethylamino)propyl)-3-ethylurea). The anhydride product rapidly hydrolyzes to its precursor state in the aqueous environment, *i.e.*, the deactivation reaction. In its finite lifetime, the hydrophobization and rigidification of the molecule can induce self-assembly or, in our design, affect the stability of a DNA hairpin. Using a copper-catalyzed alkyne−azide cycloaddition reaction, we modified an alkyne-bearing thymine to carry two carboxylates that serve as the precursor for our reaction cycle (modified thymine, Figure 1A).

First, we tested the reaction cycle's kinetics of the nucleotide itself, *i.e.*, without incorporating it in a DNA hairpin (modified thymine, Figure 1A). The addition of 4 mM EDC to 8 mM of the modified thymine in 200 mM MES at pH 6 yielded the formation of the corresponding anhydride product, as evidenced by HPLC. As the reaction progressed, the concentrations of fuel and anhydride decayed (Figure S1). The kinetics of the reaction cycle could be accurately captured with a kinetic model (see Supporting Note 1), which allowed us to calculate the half-life of the anhydride product ($t_{1/2}$) to be 23 s.

Next, we incorporated the modified thymine into a molecular beacon comprising a Cy3 dye on the 5′ end and a black hole quencher (BHQ-2) on the 3′ end of a 30-base oligomer (Figure 1B). We measured its melting temperature by fluorescence spectroscopy (see Figure S2). The molecular beacon we chose is based on a hairpin that, without any artificial modification, has a melting temperature ($T_m$) of 40.4 °C under the applied conditions (H-0, Figure 1D). We anticipated that incorporating one modified thymine would decrease the $T_m$ due to steric hindrance and electrostatic repulsion of the modified thymine compared to regular thymine. Thus, we designed H-1, which is H-0 with a point mutation of one thymine for modified thymine in the stem region of the molecular beacon. As expected, we found that its melting temperature was 10.5 °C lower than H-0. This decrease in $T_m$ was independent of where the mutation was performed (H-2), provided it was in the stem region, *i.e.*, H-3 was modified in the loop region. Its $T_m$ was almost equal to the unmodified H-0. If we added two mutations in the stem region, $T_m$ decreased by 20.6 °C (H-4, Figure 1D).

The destabilizing effect of the modified thymine can be attributed to the electrostatic repulsion of the carboxylates and/or steric hindrance of the phthalic acid and triazole in the crowded environment of the duplex. To test which of these forces was the dominant one, we synthesized the methyl ester of modified thymine which lacks the anionic nature compared to modified thymine but is similar in size (Figure 1C). When incorporated in the molecular beacon (H-5), we found a slight drop in $T_m$ (4.4 °C) compared to nonmodified H-0. This observation suggests that both a steric hindrance and the


https://doi.org/10.1021/jacs.2c08463
J. Am. Chem. Soc. XXXX, XXX, XXX−XXX

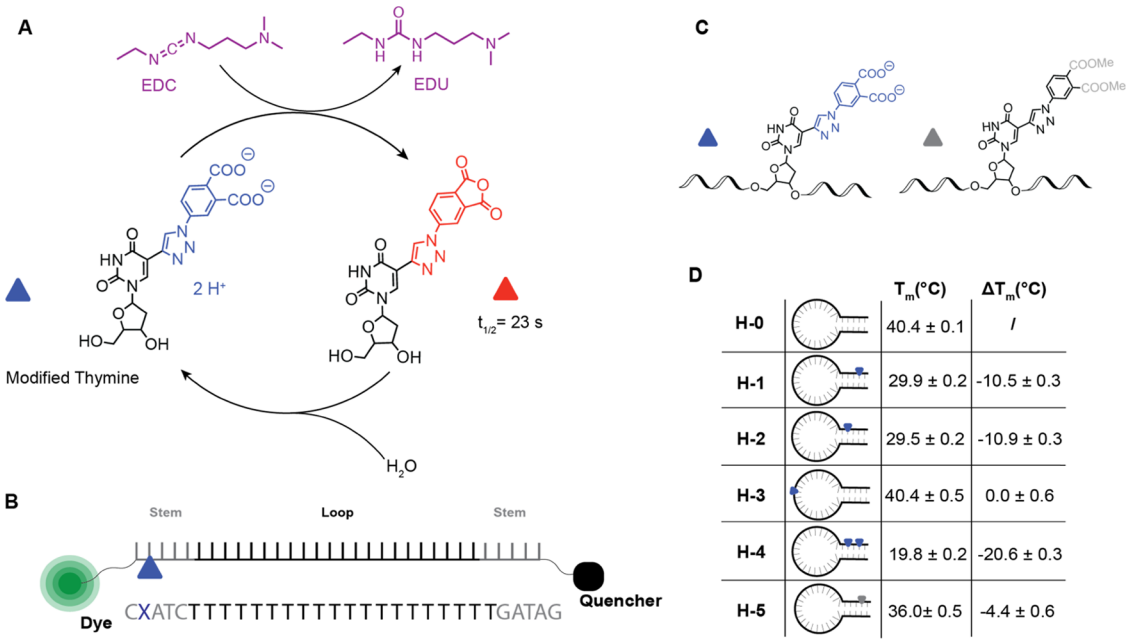


**Figure 1.** Molecular design of the dynamically folding hairpins. (A) Chemical reaction cycle activates modified thymine at the expense of a carbodiimide-based fuel. (B) Sequence of the oligomer in which the modified thymine is incorporated. The dye is Cy3, the quencher is a Black Hole Quencher 2, and the blue triangle represents the modified thymine. (C) Schematic representation of an oligomer with the modified thymine incorporated and an oligomer with a control compound, *i.e.*, the methyl ester of the modified thymine, is represented as a gray triangle. (D) Table of oligonucleotides (H-0 to H-5) with the location of their modification (blue triangles), their melting temperature ($T_m$), and the difference in $T_m$ compared to nonfunctionalized H-0 as measured by fluorescence melting experiments (see Figure S2).

presence of negative charges are responsible for the change in the $T_m$ upon incorporating modified thymine.

Next, we tested the ability of the fuel-driven chemical reaction cycle to induce the folding of the hairpin. We added 20 mM EDC to 0.2 $\mu$M H-1 (*i.e.*, a 100,000-fold excess) and monitored the fluorescence intensity of the molecular beacon as a function of time (Figure 2A,B). The experiment was performed at the $T_m$ of H-1 (30 °C). We can thus assume that roughly 50% of the hairpin was in its folded state before fuel addition. Immediately after the EDC addition, the fluorescence intensity dropped, indicating that the population of folded hairpins had increased. Ten minutes after the EDC addition, we added 10 mM *N*-acetyl aspartate (Ac-D-OH) as a scavenger, *i.e.*, a competing dicarboxylate that can also cyclically react with EDC and rapidly consume all fuel. Consequently, the hairpin fluorescence returned to a value close to the original level. We attribute the lack of a complete return due to the change in ionic strength of the solution caused by the positively charged group present in both EDC and its byproduct of hydration, *i.e.*, the waste EDU (Figure 2C).

These results suggest that adding a chemical fuel creates a steady state of anhydride, which changes the dynamic population of the folded hairpins and unfolded oligonucleotide. The reason for the high amount of fuel lies in the different rates of the reactions and the low concentration of DNA. In our reaction cycle, the activation reaction and the deactivation are simultaneously operating. The activation however follows a second-order kinetics, while the deactivation follows a pseudo-first-order kinetics. To sustain a constant level of anhydride, high enough to show a change in the population of hybridized species, we balance the effect with a great excess of fuel. We quantified the change in the folding caused by the fuel by

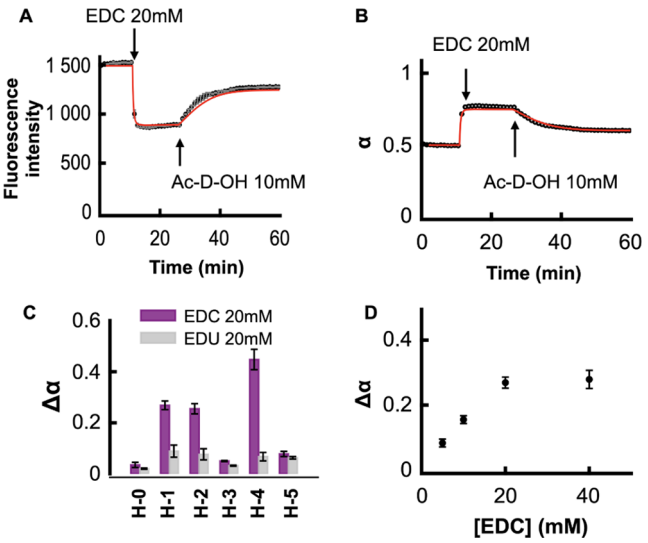


**Figure 2.** Response of the molecular beacon to chemical fuel. (A) Fluorescence intensity as a function of time for H-1. At 10 min, 20 mM EDC is added. After 15 min, 10 mM N-acetyl aspartic acid is added to consume the remaining EDC. Black markers represent the experimental data. The standard deviation of duplicate experiments is shown as an error bar. The red line represents a prediction with our kinetic model. (B) Evolution of $\alpha$ for the experiment described in panel A. (C) Comparison of the effect of fuel (EDC, 20 mM) and waste (EDU, 20 mM) on the folding of the different oligonucleotides. (D) Effect of different amounts of fuel on the folding of H-1.

calculating the amount of folded hairpins as a fraction of the total concentration of oligonucleotides ($\alpha$)

$$\alpha = \frac{[\text{folded hairpin}]}{[\text{total hairpin}]} \quad (1)$$


https://doi.org/10.1021/jacs.2c08463
J. Am. Chem. Soc. XXXX, XXX, XXX−XXX

We determined the concentration of folded hairpins by fluorescence spectroscopy by comparing the fluorescence intensity to two reference points, *i.e.*, the fluorescence intensity of a sample where all of the hairpins were folded and the fluorescence intensity at 30 °C before the addition of fuel. We prepared the sample where all of the hairpins were folded by adding 20 mM $MgCl_2$ while the corresponding $\alpha$ at 30 °C is known from the melting curve of each H (Supporting Table 1). From these two reference points, the $\alpha$ was calculated using the equation described in Supporting Notes 2.

We measured the $\alpha$ increase upon adding fuel or EDU for all of the hairpins in this work (Figure 2C). As expected, for the nonmodified hairpin H-0, the increase in $\alpha$ was minimal. Moreover, it was similar to the increase upon the addition of EDU. The same trend is observed for H-3, *i.e.*, the molecular beacon with the modified thymine in the loop region. For the final control compound, H-5, where the carboxylic acids are protected as methyl esters, the change induced by the fuel and the waste was modest. In contrast, H-1, H-2, and H-4 displayed a striking difference between adding EDC or EDU. In the case of H-4, we started with an almost open state before applying fuel ($\alpha$ = 0.21). The addition of fuel pushed the system toward a closed state ($\alpha$ = 0.66). In other words, the fuel switched the system from a condition where the open state is dominant to a new, temporary distribution where the closed state is in excess. We then explored the effect of different amounts of fuel on the folding of H-1. We chose to focus on H-1 because it has only one modified thymine, thus reducing the number of transient species. When increasing amounts of fuel are added, a greater degree of folding is achieved (Figure 2D), mainly attributed to the higher anhydride yield in a steady state. In contrast, when a similar amount of EDU was added, the change in $\alpha$ was much lower (Figure S3). These combined experiments conclude that adding fuel increases the folded hairpin population by activating the modified thymine.

The fluorescence data provided information about the overall fraction of the folded hairpin. However, precursor and activated states are simultaneously present, and each can form hairpins (see Scheme 2). Our system was designed so that the activated state is more likely to form a hairpin. We were interested in understanding the contributions of each of the two possible hairpin species to the overall fraction of folded hairpins.

We can rewrite eq 1 as the sum of two terms like in the following

$$\alpha = \frac{[\text{folded hairpins}]}{[\text{total hairpins}]} = \frac{[\text{anhydride}_{\text{folded}}] + [\text{acid}_{\text{folded}}]}{[\text{total hairpins}]}$$

$$= \frac{\alpha_1 \cdot [\text{total hairpins}] \cdot y + \alpha_0 \cdot [\text{total hairpins}] \cdot (1 - y)}{[\text{total hairpins}]}$$

$$= \alpha_1 \cdot y + \alpha_0 \cdot (1 - y)$$

where $\alpha_0$ and $\alpha_1$ are the folding ratios of the acid and the anhydride state, respectively, and $y$ is the steady-state yield of the reaction cycle. To determine those two $\alpha$ values, we thus have to determine the steady-state concentration of anhydride, which we measured by HPLC. As a precursor, we used a short oligonucleotide equipped with our modified thymine, and we applied different amounts of fuel to induce different steady-state levels. We quenched these samples after 1 min with a previously established quenching method.[50] In brief, we added EDC to a solution of unlabeled oligo (1 $\mu$M) in MES buffer at pH 5.5, and after 1 min, 2 $\mu$L of 1-pentylamine was added to the sample. We found that two new peaks appeared in the chromatogram, which we attributed to the products of the anhydride reacting with 1-pentylamine (see Figure S18). By comparing the areas of the peaks, we calculated the yield of anhydride in a steady state, which we used in our kinetic model to fit the fluorescence data as a function of time (see Supporting Note 1 and Figure S4). From the model, we derived a value for $\alpha_1$, which we estimated to be 0.95. In other words, 95% of the activated oligos are in their folded state, whereas only 50% of the nonactivated oligos are in their folded state.

The obtained data creates a clearer picture of the energy landscape of our dynamic hairpins (Scheme 2). In the energy landscapes, four states exist: a DNA strand can either be folded or unfolded, or it can either be activated or deactivated. Pathways exist between these states. However, only the eight dominant ones are shown: an unactivated strand can fold and unfold, and an activated strand can fold and unfold (pathways along the folding coordinate). Along the reaction coordinate, a folded or unfolded strand can become activated, and a folded and unfolded activated strand can become deactivated. While it is technically possible that a folded oligonucleotide simultaneously deactivates and unfolds, it is unrealistic and complicates the landscape.

We found that the activated state has a half-life of 23 s (*vide supra*). We also found that its degree of folding is in the range of 95%. Thus, in its lifetime, the activated oligomer will spend roughly 95% of its time in the folded state. However, the half-life for folding a DNA strand such as the one used in our experiments is reported to be in the range of milliseconds.[51−53] That means that even though an activated state will spend roughly 95% of its time in a folded state, it will unfold and refold 100 s of times in its lifetime.

Interestingly, the anhydride state was significantly more folded than the methyl ester control compound (activated H-1 vs H-5, $\alpha$ = 0.95 vs $\alpha$ = 0.71, under the same conditions) even though both species lack the negative charges. A possible explanation is that the formation of the anhydride increases the overall planarity of the functional group, thus facilitating intercalation and stacking into the DNA helix. We also

**Scheme 2. Proposed Energy Landscape of the Chemically Fueled Hairpin**[a]

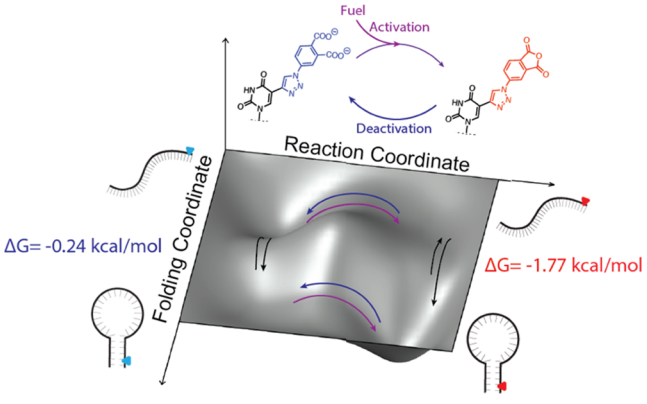


[a]A hairpin in our system can toggle between four positions in our energy landscape: unactivated and unfolded, unactivated and folded, activated and unfolded, and activated and unfolded. Chemical activation makes folding more favorable.


https://doi.org/10.1021/jacs.2c08463
J. Am. Chem. Soc. XXXX, XXX, XXX−XXX

observed a modest increase in the activation rate constant ($k_1$ in the kinetic model, see Supporting Table 2) for the modified thymine when embedded in the oligo, in agreement with the previous report from our group that a densely charged local environment can affect the reactivity of dicarboxylic acid.[41]

In the experiments above, we changed the fraction of folding of hairpins in a steady state by adding fuel. The addition of a fuel scavenger allows controlling of the steady state by rapidly depleting all fuel reversibly. Next, we introduce the idea of a permanently present fuel scavenger that consumes most fuel and thus controls the lifetime of the folded population. Such an approach opens the door to self-regulating DNA nanodevices with time-dependent behavior. When fuel is added to such a competition experiment, the majority of the fuel is consumed by the scavenger, and the conformation change of the hairpin is only temporary (Figure 3A). A simulation by our kinetic

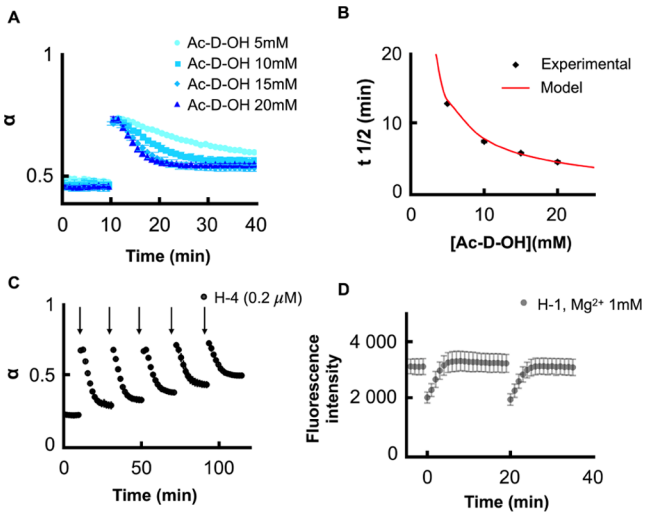


**Figure 3.** Regulating the lifetime of the folded hairpin population by introducing a fuel scavenger. (A) Variation of fraction folded ($\alpha$) of H-1 (0.2 $\mu$M fueled with 20 mM EDC) as a function of time in the presence of different amounts of Ac-D-OH (5, 10, 15, 20 mM, respectively). (B) Half-life of fluorescence recovery for experiment in (B). (C) Sequential addition of EDC 20 mM to H-4 (0.2 $\mu$M). Each purple arrow indicates one 20 mM batch of fuel addition. (D) Evolution of fluorescence signal of H-1 with 20 mM of EDC in the presence of $Mg^{2+}$1 mM and Ac-D-OH 20 mM.

model demonstrated the validity of this approach and showed that lifetimes of the folded population could be tuned from a few minutes to hours, depending on the amount of scavenger that is added (Figure 3B).

We carried out these experiments using 0.2 $\mu$M of H-1 in an MES buffer containing variable concentrations of Ac-D-OH as a scavenger at 30 °C. When 20 mM EDC was added to the system with 20 mM of scavenger, we observed a marked drop in the fluorescence, followed by a rapid signal recovery. The kinetic profile of the fluorescence recovery correlates with the experimentally determined consumption of the EDC (Figure S6). Moreover, our kinetic model accurately modeled the fluorescence signal and correlated with the predicted anhydride concentration (Figures S7 and S8). The scavenger concentration could be used to tune the half-life of recovery of the folded states from 4 min to over 13 min, in agreement with the predicted half-life of recovery (Figure 3B). The ability of the system to stop autonomously allows for operating multiple cycles with minimal intervention, which we demonstrate by adding five batches of 20 mM of EDC, which resulted in a transient change in the population of folded and unfolded molecules each time (Figure 3C). In contrast, most of the DNA dynamic system reported so far requires either extensive manipulation, such as buffer exchange, or at least two stimuli to move between the different states.

To demonstrate that our new chemically fueled hybridization can be incorporated into more sophisticated DNA structures than hairpins, we tested its resistance to magnesium ions. $Mg^{2+}$ is a critical component for the folding of DNA origami and the operation of DNA nanotechnology. We analyzed the melting curve of our model hairpin H-1 in the presence of 1 mM and 10 mM $MgCl_2$ (Figure S2). The modified thymine can still destabilize the duplex, but $\Delta T_m$ decreased to 8 from 10 °C compared to sodium-only buffer. In the case of higher concentrations of $MgCl_2$, the difference is reduced to only 1.1 °C. However, the presence of Ac-D-OH widened the window to 4.4 °C, potentially leaving a margin for operation. Aspartic acid is a weak chelator for $Mg^{2+}$ ions while stabilizing the secondary structure.[54] Lastly, we tested the response of H-1 to fuel in the presence of a low concentration of $Mg^{2+}$ (1mM) and scavenger (Figure 3D). We found the expected behavior of the fluorescence signal corresponding to transient folding.

In the first part of the work, we demonstrated the possibility of chemically fueled hybridization on a simple, unimolecular construct. In dynamic DNA nanotechnology, strand displacement is the primary strategy for actuation.[14] Thus, to demonstrate that our chemically fueled hybridization can be used to power strand displacement, we repurposed a strand displacement circuit, where a short invader strand can control the folding state of a hairpin via hybridization to the stem.[55] The chemical state of the invader (active or inactive) controls the folding state of the target, thus behaving as an actuator that converts the chemical energy of the fuel into a conformational change. We installed the modified Thymine in the inner part of the sequence (I-1, Figure 4) or at the 5′end (I-2, Figure 4). We determined the $T_m$ of the hairpin in the presence of 2 equivalents of invader strands. I-1 showed the most drastic destabilization, with a decrease of 11.4 °C of the melting temperature compared to the unmodified control I-0. On the other hand, I-2 showed only a modest decrease in the stability of the duplex due to a minor relevance of the 5′ end base to the overall 12bp duplex.

Next, we tested the system's response to chemical fuel and quantified the hairpin's degree of folding by monitoring the fluorescence intensity of the dual-labeled construct. We performed all experiments at 36 °C, i.e., above the melting temperature of I-1 and close to the $T_m$ of I-0 and I-2. The invader strand displaces the stem of the hairpin and forces it to open, increasing the fluorescence signal. Upon adding fuel, I-1 immediately shows an increase of the fraction open due to the invasion of the double-stranded region, moving from 0.13 to 0.21. The signal increases for 5 minutes and gradually decreases over 1 h. Similarly, I-2 is responsive to the fuel and induces an increase in the open fraction of the hairpin, even though it did not significantly decrease the stability of the duplex in its precursor state. The formation of the more hydrophobic anhydride likely promotes $\pi$-stacking interactions and, potentially, intercalation of planar phthalic anhydride, stabilizing the duplex even at the 5′-end. The scavenger consumes the fuel within 20 min after its addition, but an


https://doi.org/10.1021/jacs.2c08463
J. Am. Chem. Soc. XXXX, XXX, XXX−XXX

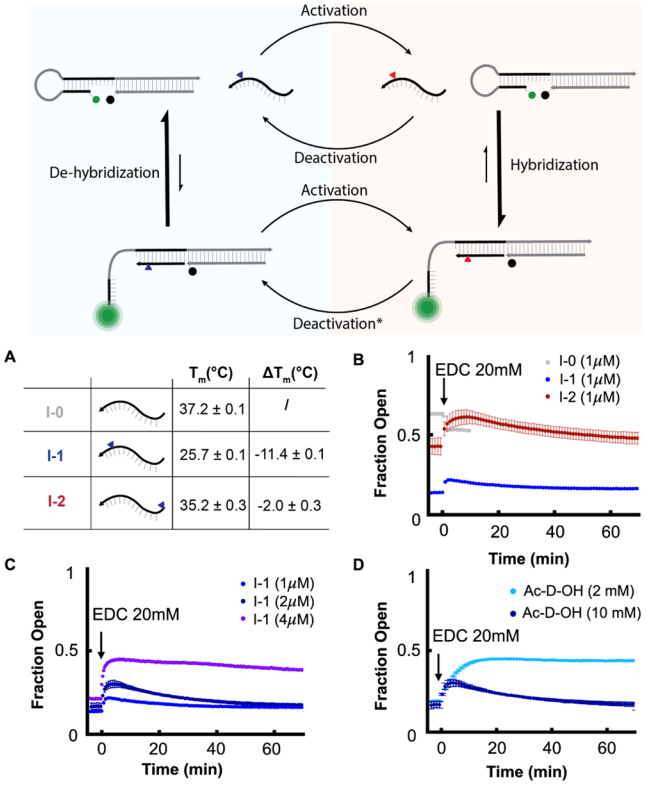


**Figure 4.** Chemically Fueled Strand Displacement. Schematic representation of the strand displacement circuit used in the experiments. (A) Melting temperature of the hairpin with invader strand (Hairpin 0.5 $\mu$M, I-1, I-2, I-0 1 $\mu$M; the melting temperature refers to the transition for the dissociation of the Hairpin-Invader duplex). (B) Evolution of open fraction of the hairpin (0.5 $\mu$M) with I-0 (1 $\mu$M, gray), I-1 (1 $\mu$M, blue), and I-2 (1 $\mu$M, red) when 20 mM of EDC are added. Buffer MES 200 mM, pH 5.6, Ac-D-OH 10 mM, ($T$ = 36 °C). (C) Evolution of the open fraction of the hairpin when an increasing amount of I-1 (1 $\mu$M blue, 2 $\mu$M dark blue, 4 $\mu$M violet) is fueled with 20 mM EDC. (D) Effect of different amounts of Ac-D-OH (10 mM dark blue, 2 mM cyan) on strand displacement with I-1 (1 $\mu$M). Measurement was performed at 36 °C. Error bars are the standard deviations of duplicate experiments.

increased fluorescence signal can still be measured until 40 min from fuel addition for I-1. Indeed, we could detect by HPLC (Figure S9) the presence of the anhydride on the strand at 40 min. The combined evidence points toward hybridization acting as a protection mechanism that slows down the anhydride hydrolysis. It further corroborates that the anhydride resides in a more hydrophobic environment, such as the bases' interface or the helix's inner part. The unmodified strand I-0, as a control, shows a permanent decrease in the open fraction of the hairpin, probably due to the change in the ionic strength of the medium caused by the fuel and waste.

We tested the effect of an increasing concentration of invader strands (Figure 4C) and a lower concentration of scavenger (Figure 4D). A higher concentration of invader strand (4 $\mu$M of I-1 instead of 1 $\mu$M) leads to a higher concentration of activated invader, which increased the open fraction of the hairpin when 20 mM of EDC was supplied (Figure 4C). Moreover, the open state persisted much longer as more anhydride can be protected by hybridization. Likewise, when the amount of scavenger is reduced from 10 mM (standard conditions) to 2 mM, the system's response to the fuel increases the efficiency of strand displacement. According to our kinetic model, the maximum yield of anhydride is only slightly higher, with a lower concentration of Ac-D-OH. However, the concentration of the active strand can be sustained for much longer since the fuel is only slowly depleted. Indeed, with 2 mM of scavenger, the open fraction increases over 15 min before plateauing (Figure 4D). In contrast, with 10 mM of scavenger, the open fraction declines after 5 min.

The strand displacement experiments above demonstrate that our chemical reaction cycle can be used to control the secondary structure of a target DNA construct by modulating the affinity of a complementary strand. In the case of the unimolecular system, there is no delay between fuel consumption and the secondary structure change. In contrast, with the bimolecular system, we have evidence of a mechanism for protecting the active state, thereby suggesting a dependence of the reaction rates of the cycle on the conformational state. In other words, the horizontal pathways in Figure 4 differ from top to bottom. The reason why the same effect is not detected on the unimolecular hairpin is most likely because of the different kinetics of unfolding. It is known that a longer duplex has slower dissociation kinetics, with half-lives that range from minutes for a 10-mer to hundreds of years for a 20-mer.[56] The hairpin used in the first part of the work has a stem of 5 bp. Therefore, the active state will constantly be exposed to the solvent because of the rapid equilibration of the hairpin between the two states. In contrast, we can expect the duplex resulting from strand invasion -12nt- not to undergo such a fast exchange, and therefore, the active state can be protected.

## CONCLUSIONS

In this work, we bridged the field of DNA nanotechnology and chemical-fueled self-assembly. We implemented a chemical reaction cycle based on a carbodiimide fuel to control the hybridization of DNA in both uni- and a bimolecular setting. We used a non-natural nucleotide functionalized with a dicarboxylic acid that undergoes the reaction cycle. The formation of the neutral and planar anhydride increases the strand's affinity for hybridization. The main difference from previous works on the autonomous or dissipative actuation of DNA is in the way energy is used.

In our work, the DNA structure plays an active role in the fuel-to-waste conversion, and the high energy state is, per se, thermodynamically not stable. In general, this approach is conceptually similar to the operational mode of biomolecular machines in the sense that the energy of a chemical fuel—an abiotic one in our case—is used to drive a conformational change of the device in a nonequilibrium fashion. The system presented in this work is not in itself a molecular machine but rather a strategy to potentially actuate DNA nanodevices in an out-of-equilibrium fashion. We envision that implementing this strategy in more complex supramolecular structures, such as DNA origami, allows us to develop machines that can convert chemical energy into work. Crucial to perform work is to overcome two challenges. First, we characterize the ratcheting constant,[57,58] which is a measure of the degree of kinetic asymmetry. In other words, we determine whether the rate of fuel consumption and deactivation change between the two states of the system. We know that the modified oligonucleotide is an active element in the dissipation process, which constitutes the first necessary requirement for kinetic asymmetry, and we have the first evidence that the rate of deactivation is lower in the hybridized state than on the free


https://doi.org/10.1021/jacs.2c08463
J. Am. Chem. Soc. XXXX, XXX, XXX−XXX

strand. Additionally, the carbodiimide reaction cycle has proven successful in operating information ratchets[44−46,59] that are fundamentally based on kinetic asymmetry. The second challenge is related to the operational conditions of the system. The activation of a single modification induces a moderate change in the melting temperature, but the coupling of several modifications strategically placed in a modular object, such as a DNA Origami, would multiply the effect upon activation. The presence of divalent cations required for DNA Origami, which is detrimental for our system, can be avoided by stabilization of the nanostructure to survive at low-ionic strength environments[60−63] better suited for the effective performance of our reaction cycle. Taken together, we will install multiple modified thymines in DNA nanostructures to develop a machine that converts chemical energy into work.

## ■ ASSOCIATED CONTENT

### Supporting Information

The Supporting Information is available free of charge at https://pubs.acs.org/doi/10.1021/jacs.2c08463.

Materials and methods description, additional fluorescence data, and HPLC data (PDF)

## ■ AUTHOR INFORMATION


### Corresponding Author

**Job Boekhoven** − *School of Natural Sciences, Department of Chemistry, Technical University of Munich, Garching 85748, Germany*; orcid.org/0000-0002-9126-2430; Email: job.boekhoven@tum.de

### Authors

**Michele Stasi** − *School of Natural Sciences, Department of Chemistry, Technical University of Munich, Garching 85748, Germany*

**Alba Monferrer** − *School of Natural Sciences, Department of Physics, Technical University of Munich, Garching 85748, Germany; Munich Institute of Biomedical Engineering, Technical University of Munich, Garching 85748, Germany*

**Leon Babl** − *Max Planck Institute of Biochemistry, Martinsried 82152, Germany*

**Sreekar Wunnava** − *Center for NanoScience (CeNS) and Systems Biophysics, Ludwig-Maximilian University Munich, Munich 80799, Germany*

**Christina Felicitas Dirscherl** − *Center for NanoScience (CeNS) and Systems Biophysics, Ludwig-Maximilian University Munich, Munich 80799, Germany*

**Dieter Braun** − *Center for NanoScience (CeNS) and Systems Biophysics, Ludwig-Maximilian University Munich, Munich 80799, Germany*; orcid.org/0000-0001-7751-1448

**Petra Schwille** − *Max Planck Institute of Biochemistry, Martinsried 82152, Germany*; orcid.org/0000-0002-6106-4847

**Hendrik Dietz** − *School of Natural Sciences, Department of Physics, Technical University of Munich, Garching 85748, Germany; Munich Institute of Biomedical Engineering, Technical University of Munich, Garching 85748, Germany*; orcid.org/0000-0003-1270-3662

Complete contact information is available at: https://pubs.acs.org/10.1021/jacs.2c08463


### Author Contributions

The manuscript was written through the contributions of all authors. All authors have approved the final version of the manuscript.

### Notes

The authors declare no competing financial interest.

## ■ ACKNOWLEDGMENTS

J.B. and H.D. are grateful for support from the TUM Innovation Network—RISE, funded through the Excellence Strategy. This research was conducted within the Max Planck School Matter to Life, supported by the German Federal Ministry of Education and Research (BMBF) in collaboration with the Max Planck Society. J.B. is grateful for funding from the European Research Council (ERC Starting Grant 852187) and the Deutsche Forschungsgemeinschaft (DFG, German Research Foundation) under Germany's Excellence Strategy—EXC-2094—390783311 and project 411722921. H.D. is grateful for funding from the European Research Council (ERC Consolidator Grant 724261). This project has received funding from the European Union's Horizon 2020 Research and Innovation Program under the Marie Skłodowska-Curie Grant Agreement No. 765703 (to H.D. and A.M.). J.B. is grateful for an extensive discussion with R. Dean Astumian (Univ. Maine).

## ■ ABBREVIATIONS USED

| | |
|---|---|
| EDC | 1-ethyl-3-(3-dimethylaminopropyl) carbodiimide |
| EDU | 1-(3-(dimethylamino)propyl)-3-ethylurea |
| Ac-D-OH | *N*-acetyl aspartic acid |

## ■ REFERENCES


(1) Rothemund, P. W. K. Folding DNA to create nanoscale shapes and patterns. *Nature* **2006**, *440*, 297−302.

(2) Douglas, S. M.; Dietz, H.; Liedl, T.; Högberg, B.; Graf, F.; Shih, W. M. Self-assembly of DNA into nanoscale three-dimensional shapes. *Nature* **2009**, *459*, 414−418.

(3) Dietz, H.; Douglas, S. M.; Shih, W. M. Folding DNA into Twisted and Curved Nanoscale Shapes. *Science* **2009**, *325*, 725.

(4) Hong, F.; Zhang, F.; Liu, Y.; Yan, H. DNA Origami: Scaffolds for Creating Higher Order Structures. *Chem. Rev.* **2017**, *117*, 12584−12640.

(5) Dong, J.; Zhou, C.; Wang, Q. Towards Active Self-Assembly Through DNA Nanotechnology. *Top. Curr. Chem.* **2020**, *378*, No. 33.

(6) Teller, C.; Willner, I. Functional nucleic acid nanostructures and DNA machines. *Curr. Opin. Biotechnol.* **2010**, *21*, 376−391.

(7) Ramezani, H.; Dietz, H. Building machines with DNA molecules. *Nat. Rev. Genet.* **2020**, *21*, 5−26.

(8) Gerling, T.; Wagenbauer, K. F.; Neuner, A. M.; Dietz, H. Dynamic DNA devices and assemblies formed by shape-complementary, non−base pairing 3D components. *Science* **2015**, *347*, 1446.

(9) Pumm, A.-K.; Engelen, W.; Kopperger, E.; Isensee, J.; Vogt, M.; Kozina, V.; Kube, M.; Honemann, M. N.; Bertosin, E.; Langecker, M.; Golestanian, R.; Simmel, F. C.; Dietz, H. A DNA origami rotary ratchet motor. *Nature* **2022**, *607*, 492−498.

(10) Bertosin, E.; Maffeo, C. M.; Drexler, T.; Honemann, M. N.; Aksimentiev, A.; Dietz, H. A nanoscale reciprocating rotary mechanism with coordinated mobility control. *Nat. Commun.* **2021**, *12*, No. 7138.

(11) Zhang, D. Y.; Winfree, E. Control of DNA Strand Displacement Kinetics Using Toehold Exchange. *J. Am. Chem. Soc.* **2009**, *131*, 17303−17314.

(12) Simmel, F. C.; Yurke, B.; Singh, H. R. Principles and Applications of Nucleic Acid Strand Displacement Reactions. *Chem. Rev.* **2019**, *119*, 6326−6369.

(13) Li, J.; Johnson-Buck, A.; Yang, Y. R.; Shih, W. M.; Yan, H.; Walter, N. G. Exploring the speed limit of toehold exchange with a cartwheeling DNA acrobat. *Nat. Nanotechnol.* **2018**, *13*, 723−729.
(14) Zhang, D. Y.; Seelig, G. Dynamic DNA nanotechnology using strand-displacement reactions. *Nat. Chem.* **2011**, *3*, 103−113.
(15) Del Grosso, E.; Ragazzon, G.; Prins, L. J.; Ricci, F. Fuel-Responsive Allosteric DNA-Based Aptamers for the Transient Release of ATP and Cocaine. *Angew. Chem., Int. Ed.* **2019**, *58*, 5582−5586.
(16) Gentile, S.; Del Grosso, E.; Prins, L. J.; Ricci, F. Reorganization of Self-Assembled DNA-Based Polymers using Orthogonally Addressable Building Blocks. *Angew. Chem., Int. Ed.* **2021**, *60*, 12911−12917.
(17) Groeer, S.; Walther, A. Switchable supracolloidal 3D DNA origami nanotubes mediated through fuel/antifuel reactions. *Nanoscale* **2020**, *12*, 16995−17004.
(18) Kuzyk, A.; Yang, Y.; Duan, X.; Stoll, S.; Govorov, A. O.; Sugiyama, H.; Endo, M.; Liu, N. A light-driven three-dimensional plasmonic nanosystem that translates molecular motion into reversible chiroptical function. *Nat. Commun.* **2016**, *7*, No. 10591.
(19) Del Grosso, E.; Ponzo, I.; Ragazzon, G.; Prins, L. J.; Ricci, F. Disulfide-Linked Allosteric Modulators for Multi-cycle Kinetic Control of DNA-Based Nanodevices. *Angew. Chem., Int. Ed.* **2020**, *59*, 21058−21063.
(20) Del Grosso, E.; Prins, L. J.; Ricci, F. Transient DNA-Based Nanostructures Controlled by Redox Inputs. *Angew. Chem., Int. Ed.* **2020**, *59*, 13238−13245.
(21) Göpfrich, K.; Urban, M. J.; Frey, C.; Platzman, I.; Spatz, J. P.; Liu, N. Dynamic Actuation of DNA-Assembled Plasmonic Nanostructures in Microfluidic Cell-Sized Compartments. *Nano Lett.* **2020**, *20*, 1571−1577.
(22) Heinen, L.; Walther, A. Temporal control of i-motif switch lifetimes for autonomous operation of transient DNA nanostructures. *Chem. Sci.* **2017**, *8*, 4100−4107.
(23) Mariottini, D.; Del Giudice, D.; Ercolani, G.; Di Stefano, S.; Ricci, F. Dissipative operation of pH-responsive DNA-based nanodevices. *Chem. Sci.* **2021**, *12*, 11735−11739.
(24) Marras, A. E.; Shi, Z.; Lindell, M. G.; Patton, R. A.; Huang, C.-M.; Zhou, L.; Su, H.-J.; Arya, G.; Castro, C. E. Cation-Activated Avidity for Rapid Reconfiguration of DNA Nanodevices. *ACS Nano* **2018**, *12*, 9484−9494.
(25) Lauback, S.; Mattioli, K. R.; Marras, A. E.; Armstrong, M.; Rudibaugh, T. P.; Sooryakumar, R.; Castro, C. E. Real-time magnetic actuation of DNA nanodevices via modular integration with stiff micro-levers. *Nat. Commun.* **2018**, *9*, No. 1446.
(26) Kopperger, E.; List, J.; Madhira, S.; Rothfischer, F.; Lamb, D. C.; Simmel, F. C. A self-assembled nanoscale robotic arm controlled by electric fields. *Science* **2018**, *359*, 296−301.
(27) Ranallo, S.; Sorrentino, D.; Ricci, F. Orthogonal regulation of DNA nanostructure self-assembly and disassembly using antibodies. *Nat. Commun.* **2019**, *10*, No. 5509.
(28) Green, L. N.; Subramanian, H. K. K.; Mardanlou, V.; Kim, J.; Hariadi, R. F.; Franco, E. Autonomous dynamic control of DNA nanostructure self-assembly. *Nat. Chem.* **2019**, *11*, 510−520.
(29) Yehl, K.; Mugler, A.; Vivek, S.; Liu, Y.; Zhang, Y.; Fan, M.; Weeks, E. R.; Salaita, K. High-speed DNA-based rolling motors powered by RNase H. *Nat. Nanotechnol.* **2016**, *11*, 184−190.
(30) Deng, J.; Walther, A. Fuel-Driven Transient DNA Strand Displacement Circuitry with Self-Resetting Function. *J. Am. Chem. Soc.* **2020**, *142*, 21102−21109.
(31) Deng, J.; Walther, A. Pathway Complexity in Fuel-Driven DNA Nanostructures with Autonomous Reconfiguration of Multiple Dynamic Steady States. *J. Am. Chem. Soc.* **2020**, *142*, 685−689.
(32) Feng, Y.; Ovalle, M.; Seale, J. S. W.; Lee, C. K.; Kim, D. J.; Astumian, R. D.; Stoddart, J. F. Molecular Pumps and Motors. *J. Am. Chem. Soc.* **2021**, *143*, 5569−5591.
(33) Del Grosso, E.; Franco, E.; Prins, L. J.; Ricci, F. Dissipative DNA nanotechnology. *Nat. Chem.* **2022**, *14*, 600−613.
(34) Deng, J.; Walther, A. Autonomous DNA nanostructures instructed by hierarchically concatenated chemical reaction networks. *Nat. Commun.* **2021**, *12*, No. 5132.
(35) Deng, J.; Liu, W.; Sun, M.; Walther, A. Dissipative Organization of DNA Oligomers for Transient Catalytic Function. *Angew. Chem., Int. Ed.* **2022**, *61*, No. e202113477.
(36) Deng, J.; Walther, A. Programmable ATP-Fueled DNA Coacervates by Transient Liquid-Liquid Phase Separation. *Chem* **2020**, *6*, 3329−3343.
(37) Del Grosso, E.; Irmisch, P.; Gentile, S.; Prins, L. J.; Seidel, R.; Ricci, F. Dissipative Control over the Toehold-Mediated DNA Strand Displacement Reaction. *Angew. Chem., Int. Ed.* **2022**, *61*, No. e202201929.
(38) Boekhoven, J.; Hendriksen, W. E.; Koper, G. J.; Eelkema, R.; van Esch, J. H. Transient assembly of active materials fueled by a chemical reaction. *Science* **2015**, *349*, 1075−1079.
(39) Tena-Solsona, M.; Riess, B.; Grotsch, R. K.; Lohrer, F. C.; Wanzke, C.; Kasdorf, B.; Bausch, A. R.; Muller-Buschbaum, P.; Lieleg, O.; Boekhoven, J. Non-equilibrium dissipative supramolecular materials with a tunable lifetime. *Nat. Commun.* **2017**, *8*, No. 15895.
(40) Dai, K.; Fores, J. R.; Wanzke, C.; Winkeljann, B.; Bergmann, A. M.; Lieleg, O.; Boekhoven, J. Regulating Chemically Fueled Peptide Assemblies by Molecular Design. *J. Am. Chem. Soc.* **2020**, *142*, 14142−14149.
(41) Kriebisch, B. A. K.; Jussupow, A.; Bergmann, A. M.; Kohler, F.; Dietz, H.; Kaila, V. R. I.; Boekhoven, J. Reciprocal Coupling in Chemically Fueled Assembly: A Reaction Cycle Regulates Self-Assembly and Vice Versa. *J. Am. Chem. Soc.* **2020**, *142*, 20837−20844.
(42) Späth, F.; Donau, C.; Bergmann, A. M.; Kranzlein, M.; Synatschke, C. V.; Rieger, B.; Boekhoven, J. Molecular Design of Chemically Fueled Peptide-Polyelectrolyte Coacervate-Based Assemblies. *J. Am. Chem. Soc.* **2021**, *143*, 4782−4789.
(43) Wanzke, C.; Jussupow, A.; Kohler, F.; Dietz, H.; Kaila, V. R. I.; Boekhoven, J. Dynamic Vesicles Formed By Dissipative Self-Assembly. *ChemSystemsChem* **2020**, *2*, No. e1900044.
(44) Borsley, S.; Leigh, D. A.; Roberts, B. M. W. A Doubly Kinetically-Gated Information Ratchet Autonomously Driven by Carbodiimide Hydration. *J. Am. Chem. Soc.* **2021**, *143*, 4414−4420.
(45) Borsley, S.; Kreidt, E.; Leigh, D. A.; Roberts, B. M. W. Autonomous fuelled directional rotation about a covalent single bond. *Nature* **2022**, *604*, 80−85.
(46) Borsley, S.; Leigh, D. A.; Roberts, B. M. W.; Vitorica-Yrezabal, I. J. Tuning the Force, Speed, and Efficiency of an Autonomous Chemically Fueled Information Ratchet. *J. Am. Chem. Soc.* **2022**, *144*, 17241−17248.
(47) Kariyawasam, L. S.; Hartley, C. S. Dissipative Assembly of Aqueous Carboxylic Acid Anhydrides Fueled by Carbodiimides. *J. Am. Chem. Soc.* **2017**, *139*, 11949−11955.
(48) Schnitter, F.; Bergmann, A. M.; Winkeljann, B.; Rodon Fores, J.; Lieleg, O.; Boekhoven, J. Synthesis and characterization of chemically fueled supramolecular materials driven by carbodiimide-based fuels. *Nat. Protoc.* **2021**, *16*, 3901−3932.
(49) Tena-Solsona, M.; Janssen, J.; Wanzke, C.; Schnitter, F.; Park, H.; Rieß, B.; Gibbs, J. M.; Weber, C. A.; Boekhoven, J. Accelerated Ripening in Chemically Fueled Emulsions**. *ChemSystemsChem* **2021**, *3*, No. e2000034.
(50) Schnitter, F.; Boekhoven, J. A Method to Quench Carbodiimide-Fueled Self-Assembly. *ChemSystemsChem* **2021**, *3*, No. e2000037.
(51) Tsukanov, R.; Tomov, T. E.; Berger, Y.; Liber, M.; Nir, E. Conformational Dynamics of DNA Hairpins at Millisecond Resolution Obtained from Analysis of Single-Molecule FRET Histograms. *J. Phys. Chem. B* **2013**, *117*, 16105−16109.
(52) Wallace, M. I.; Ying, L.; Balasubramanian, S.; Klenerman, D. Non-Arrhenius kinetics for the loop closure of a DNA hairpin. *Proc. Natl. Acad. of Sci. U.S.A.* **2001**, *98*, 5584−5589.
(53) Grunwell, J. R.; Glass, J. L.; Lacoste, T. D.; Deniz, A. A.; Chemla, D. S.; Schultz, P. G. Monitoring the Conformational


https://doi.org/10.1021/jacs.2c08463
J. Am. Chem. Soc. XXXX, XXX, XXX−XXX

Fluctuations of DNA Hairpins Using Single-Pair Fluorescence Resonance Energy Transfer. *J. Am. Chem. Soc.* **2001**, *123*, 4295−4303.
(54) Yamagami, R.; Bingaman, J. L.; Frankel, E. A.; Bevilacqua, P. C. Cellular conditions of weakly chelated magnesium ions strongly promote RNA stability and catalysis. *Nat. Commun.* **2018**, *9*, No. 2149.
(55) Adam, V.; Prusty, D. K.; Centola, M.; Škugor, M.; Hannam, J. S.; Valero, J.; Klöckner, B.; Famulok, M. Expanding the Toolbox of Photoswitches for DNA Nanotechnology Using Arylazopyrazoles. *Chem. − Eur. J.* **2018**, *24*, 1062−1066.
(56) Morrison, L. E.; Stols, L. M. Sensitive fluorescence-based thermodynamic and kinetic measurements of DNA hybridization in solution. *Biochemistry* **1993**, *32*, 3095−3104.
(57) Astumian, R. D. Kinetic asymmetry allows macromolecular catalysts to drive an information ratchet. *Nat. Commun.* **2019**, *10*, No. 3837.
(58) Das, K.; Gabrielli, L.; Prins, L. J. Chemically Fueled Self-Assembly in Biology and Chemistry. *Angew. Chem., Int. Ed.* **2021**, *60*, 20120−20143.
(59) Mo, K.; Zhang, Y.; Dong, Z.; Yang, Y.; Ma, X.; Feringa, B. L.; Zhao, D. Intrinsically unidirectional chemically fuelled rotary molecular motors. *Nature* **2022**, *609*, 293−298.
(60) Bertosin, E.; Stömmer, P.; Feigl, E.; Wenig, M.; Honemann, M. N.; Dietz, H. Cryo-Electron Microscopy and Mass Analysis of Oligolysine-Coated DNA Nanostructures. *ACS Nano* **2021**, *15*, 9391−9403.
(61) Ponnuswamy, N.; Bastings, M. M. C.; Nathwani, B.; Ryu, J. H.; Chou, L. Y. T.; Vinther, M.; Li, W. A.; Anastassacos, F. M.; Mooney, D. J.; Shih, W. M. Oligolysine-based coating protects DNA nanostructures from low-salt denaturation and nuclease degradation. *Nat. Commun.* **2017**, *8*, No. 15654.
(62) Gerling, T.; Kube, M.; Kick, B.; Dietz, H. Sequence-programmable covalent bonding of designed DNA assemblies. *Sci. Adv.* **2018**, *4*, No. eaau1157.
(63) Rajendran, A.; Endo, M.; Katsuda, Y.; Hidaka, K.; Sugiyama, H. Photo-Cross-Linking-Assisted Thermal Stability of DNA Origami Structures and Its Application for Higher-Temperature Self-Assembly. *J. Am. Chem. Soc.* **2011**, *133*, 14488−14491.


https://doi.org/10.1021/jacs.2c08463
*J. Am. Chem. Soc.* XXXX, XXX, XXX−XXX